

Ground-testing of One-way Ranging from a Lunar Beacon Demonstrator Payload (Lunar Node -1)

Evan J Anzalone, Jacob Jensen, Tamara L. Statham, *NASA/Marshall Space Flight Center*

Scott H. Bryant, Kathleen A. Harmon, *NASA/Jet Propulsion Laboratory*

Greg Lee, *Tethers Unlimited, Inc*

Mike G. Abbod, Randy E. Barter, Albert Ibarra, Timothy J. Hoffman, Lorenzo L. Morgan, Ricky D. Overcash, Collin J. Rokke, *Peraton Inc.*

BIOGRAPHY (IES)

Evan Anzalone and Tamara Statham are the PI and Co-I for the LN-1 mission, supporting Guidance, Navigation, and Mission Design at Marshall Space Flight Center within EV42. Jacob Jensen is a member of the LN-1 team with primary responsibility for digital logic design and testing.

Scott Bryant is a member of the Senior Staff at the NASA Caltech Jet Propulsion Laboratory. He is the tracking subsystem engineer for DSN implementations, and the Cognizant Design Engineer for the DSN Ranging system. Kathleen Hamon is a senior systems engineer at the NASA Caltech Jet Propulsion Laboratory in Pasadena, California, focusing on mission and ground systems. She currently works as a Mission Interface Manager for NASA's Deep Space Network.

Gregory Lee is the Sr. RF Architect at Tethers Unlimited where he is responsible for developing and supporting their line of software defined radios and new radio frequency assemblies.

The Peraton test team is comprised of engineers working on the NASA-JPL DSN O&M Contract. Most of the Compatibility Test team were test engineers in the IT&A group, led by lead engineer Collin Rokke. The operational preparations and planning were spearheaded by the Network Operations Project Engineer for this mission, Tim Hofmann. Additional engineers from the Peraton support team include Randy Barter, Ricky Overcash, and Mike Abbod.

ABSTRACT

Similar to lighthouses providing navigation aids and awareness to ships sailing along the coast, in-situ navigation beacons can be used to provide redundancy, awareness, and improved onboard position knowledge for vehicles operating in and around the lunar sphere of influence. Lunar Node - 1 is a radio frequency navigation beacon that is manifested on Intuitive Machines' NOVA-C lunar lander flight in 2022 for operation during cruise and from a mid-latitude landing location. This payload utilizes commercial components developed for Low Earth Orbit applications and packages them into an integrated package to provide a navigation reference signal as part of a large lunar-centric navigation network. As part of its operations, Deep Space Network ground stations will operate as the notional "user" of this service, allowing for performance characterization, calibration, and operation of the beacon payload. This paper provides an overview of the payload, how its fits into a large concept of operations, and ground testing results. A specific focus is on ground testing of the payload with DSN ground receivers as part of Radio Frequency (RF) Compatibility Testing. A primary goal of this testing was to characterize a pseudo-noise ranging code sequence generated by the payload. The results in this paper define the testing sequence, unique operational constraints with two-way ranging ground equipment, and applications of the ground-derived error model to predicted in-flight performance of the ranging code.

INTRODUCTION

Description of approach for lunar architecture and the need for PNT support and approach for prior support. -Evan With the recent heavy investment in missions targeting lunar space, both on the surface and in various orbits [1], cislunar space will be approaching a critical mass where the number of vehicles and support assets operating simultaneously is large enough that the desire for in-situ aids becomes preferable to independent fully Earth-centric operations. There have been studies previous in ideas of the Interplanetary Internet [2] and concepts like LunaNet [3] which seeks to build out a more robust network to enable multi-user compatibility and a shared backbone of data to/from Earth. This is not only for communication and data

transport, but also areas such as navigation. The baseline approach for long-term lunar orbiting assets and for the Apollo missions was to utilize ground-tracking assets on Earth to provide updates to vehicles of its position and velocity at a given time [4,5]. While this approach is well understood and implemented, it is limited by the number of available ground stations and support observations. Scenarios such as multi-spacecraft in a network help to alleviate this impact, but with increasing missions requiring high data simultaneously, alternate solutions are needed for long-term sustainability and growth.

One approach to inter-asset navigation within a distributed network is the Multi-spacecraft Autonomous Positioning System (MAPS) [6]. In this concept, each spacecraft shares its timing and state knowledge as part of either system broadcasts or pre-programmed communication passes within the network. A Concepts of Operations is given in Figure 1 below. In this approach, the relays operating as trunks on each planetary network act as anchors, providing high accuracy timing and state references to other elements throughout the network. With this approach, digital information embedded into the communication packet standard allows for sharing of navigation information as part of every communication link between assets.

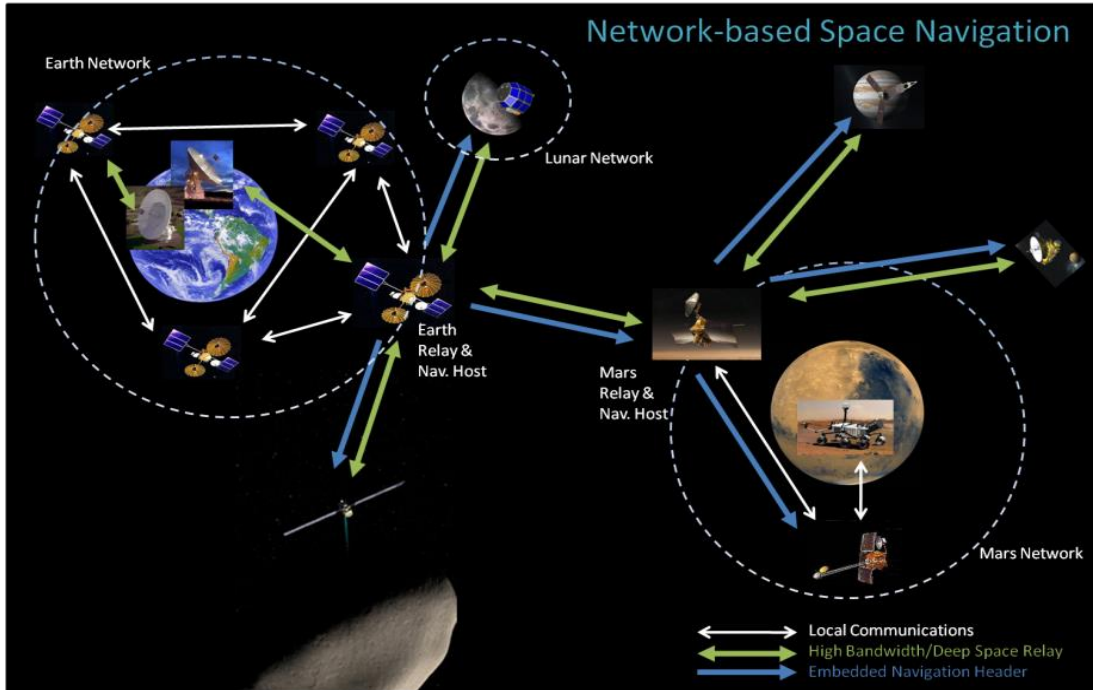


Figure 1. MAPS Concept of Operations

This concept has studied in paper studies as well as software testing using the Software Defined Radio Testbed was on the International Space Station [7]. This technology and approach provides an opportunity to demonstrate and improve local navigation around the moon. This concept, along with influences from other navigation approaches forms the basis of the Lunar Node – 1 Payload [8].

LUNAR NODE – 1

Lunar Node 1 (LN-1) is an S-band navigation beacon for lunar applications that was recently designed, built, and tested at MSFC. As part of NASA's Commercial Lunar Payload Service initiative, this beacon, shown in Figure 2, will be delivered to the Moon's surface on Intuitive Machine's NOVA-C lunar lander in 2022.

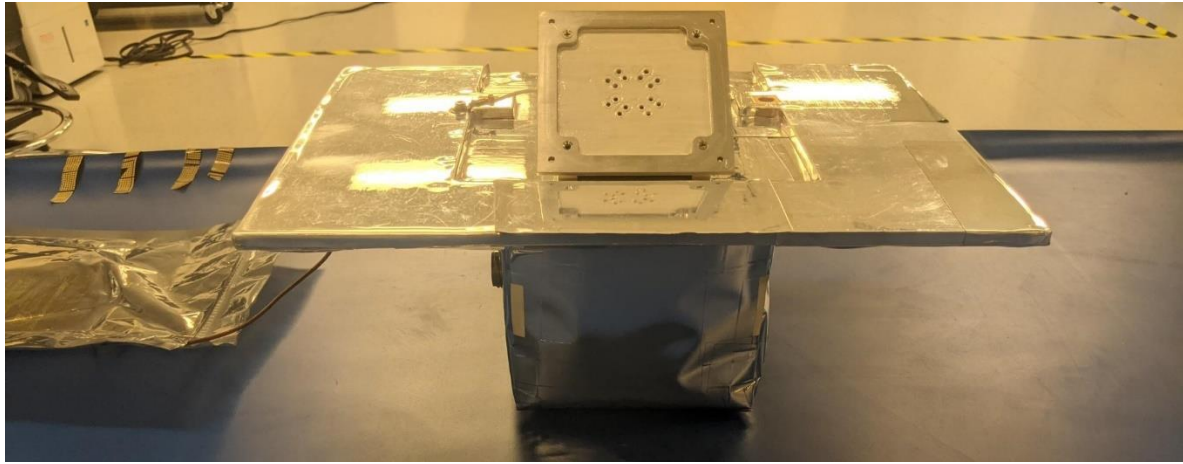


Figure 2: Lunar Node -1 Payload at Host Integration Facility (w/ antenna hat mounting bracket)

During this mission, LN-1 has a goal to demonstrate navigation technologies that can support local surface and orbital operations around the moon, enabling a new autonomy capability which would decrease dependency on heavily utilized Earth based assets like the Deep Space Network. An additional goal is to demonstrate and raise understanding of constraints, issues, and operational approaches to management of lunar navigation aids from Earth.

To reach these goals, LN-1's design leverages Cubesat components as well as the MAPS algorithms, which enable the autonomous spacecraft positioning through communication-integrated navigation measurements. In addition to demonstrating the MAPS approach, the radio will also be used in PN-based one-way non-coherent ranging and Doppler tracking to provide alternate approaches and comparisons for navigation performance. LN-1 will represent a single node in a potential greater MAPS network of assets aiding the development of lunar architectures. A representation of this network can be seen in Figure 3.

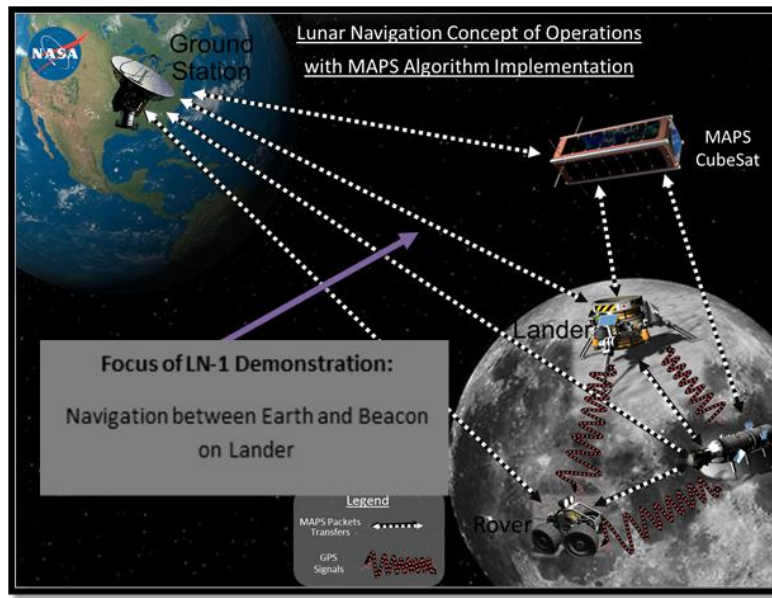


Figure 3. LN-1 Concept of Operations

Payload Description and Objectives

LN-1 will need to demonstrate that its packets can be successfully received and processed to determine the payload state. To do this, over the course of the 7-day trans-lunar cruise and 13.5 earth days of lunar surface operations, LN-1 will broadcast out its state and timing information back to Earth for several observation passes to the Deep Space Network (DSN). Upon reception of this data, high accuracy packet reception timestamps will be used (along with atmospheric data for induced delays) to assess a ranging observation. This data will be captured across multiple passes to compute a navigation state of the payload over the mission. In addition to demonstrating the MAPS payload, the radio will also be used in PN-based one-way non-coherent ranging and Doppler tracking to provide alternate approach for navigation performance. In anticipation of next year's landing on the lunar surface, the team is also working to develop potential collaborations including cross-link demonstrations with potential VLBI-earth based observations. Further, the team is also working to bring additional ground stations online to get raw Radio Frequency observations to aid in development of one-way PN receivers.

An innovative aspect to LN-1 is that it provides a modular design, made with commercial off the shelf (COTS) components, that could be integrated into a variety of host vehicles and, with adequate power generation/storage, be able to offer long-term operation. Future host vehicles can include satellites, rovers, and landers that are part of a greater lunar architecture. Figure 4, which shows the flight payload, the compact size of the spacecraft can be identified. In terms of dimensions, the primary structure is approximately 175x220x300 cm in volume and ~2.8kg in mass. The dominating factor of the design is the large top surface which is the spacecraft's radiator. To provide a clean interface with the host vehicle, LN-1 has designed a radiator to allow for heat dumping during operation. This is needed due to the hot environment on the lunar surface at lunar noon, combined with the heat generated by the power draw of the radio while transmitting.

The primary components of LN-1 can be identified in the cutaway drawing in the engineering drawing cutaway. The vertical board provides the primary interface and power regulation to the payload, with the remaining electrical components on the horizontal board. This package includes the ACTEL FPGA computing element, the Space-rated CSAC, and the interface to the radio. The SWIFT SLX transmitter is mounted underneath the radiator of the payload to allow for maximum heat dissipation during operations. The antenna is mounted on a 45 degree bracket to allow for improved pointing of the payload to the Earth with expected flight vehicle pointing and expected direction to Earth from the landing site.

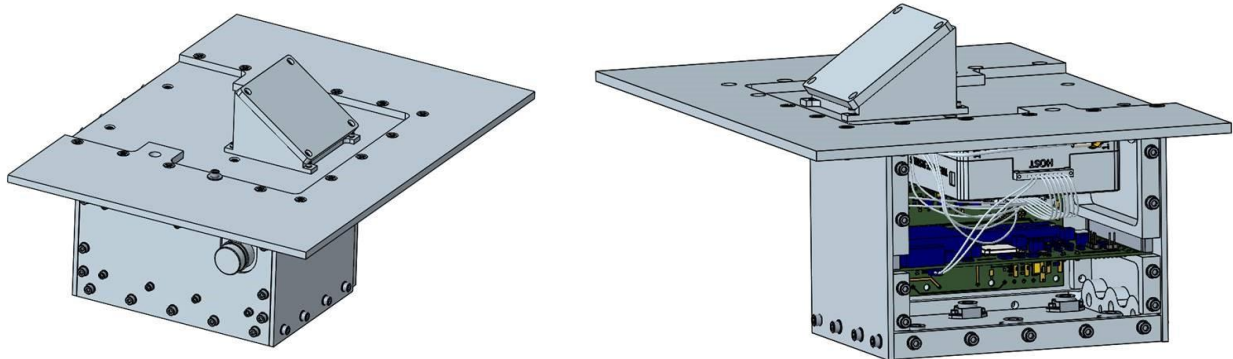


Figure 4. External and Cutaway View of LN-1

Flight Operations Plan

As part of the flight demonstration, LN-1 will operate as an independent radio transmitter on the host vehicle. The Concept of Operations of the payload is given in the left bracket in Figure 5 below. For all navigation modes being tested, the payload will operate concurrently with transmission from the host vehicle. The connection between the payload and host lander is via RS-422 over the lander's communication network. LN-1 will use this connection for payload commanding and tracking health and status. This interface will be used to track how well the payload can sync its clock and information to the onboard (and ground-corrected) timing information as well as verify transmission status and packet generation. Telemetry generated by the payload will be received by an independent set of ground stations that will perform data recording and processing. This includes timestamping of all telemetry data, Doppler observations, and one-way ranging measurements. For this application, the Deep Space Network was selected as the ground station to stand in for a notional user. The DSN was selected due to the need for large receive dishes to meet payload link margin requirements, as well as for the sophisticated and proven interface with flight

navigation products for deep space. This will allow the team to process and perform orbit determination using standard DSN tools, such as the MONTE[9] package to provide a flight-like scenario and analysis backend.

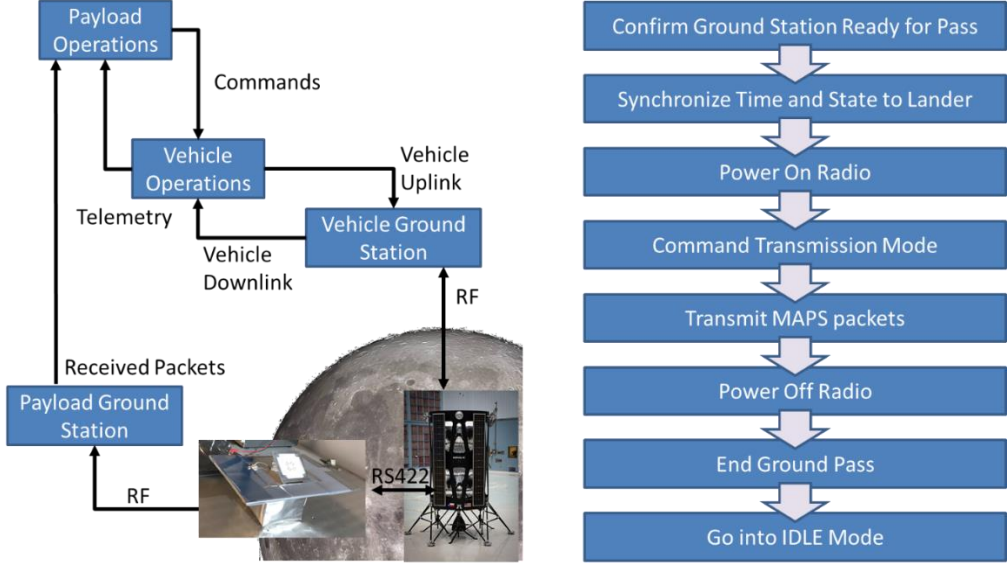


Figure 5. Concept of Operations

Flight Radio Transmitter

LN-1's transmission capability is provided by a SWIFT SLX. The SWIFT-SLX radio system is a high performance relatively low cost software defined radio designed by Tethers Unlimited and flown by a number of different customers in low earth orbit primarily being used as a flight telemetry command and control radio link. The SWIFT-SLX hardware is segmented into two different slices. Each SWIFT radio contains a baseband processor card and an RF front end slice. The baseband processor card contains the host interface, VCXO crystal oscillator, clock distribution network, high speed 14 bit analog to digital and digital to analog converters. The system is designed to be able to interface with traditional reference clock inputs used in satellite communications. Shown below in Figure 6 is the baseband clocking architecture.

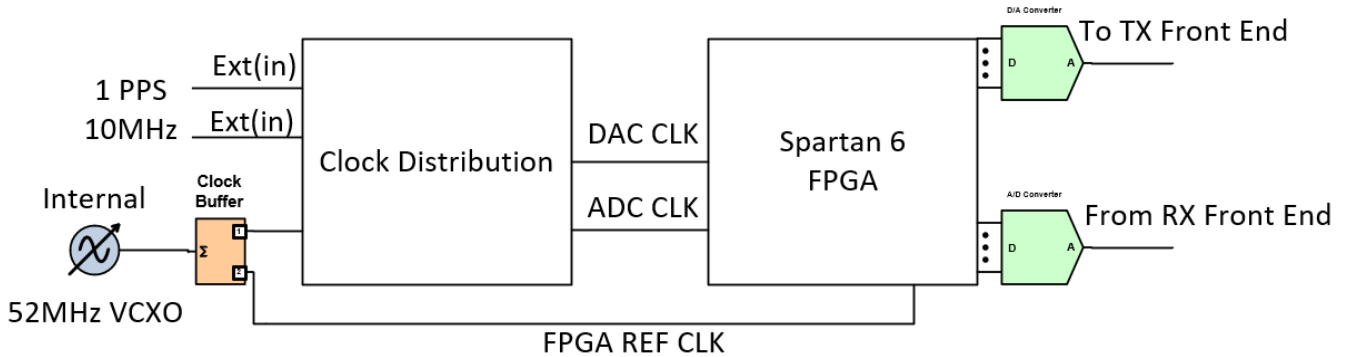


Figure 6: SWIFT-SLX Baseband Clocking Architecture.

The internal VCXO can be synced with both a 1PPS and a 10MHz external reference input signal. For LN-1's operation, the radio is synced to the onboard timing signal generated by the Space CSAC (which is capable of generating both a 1 PPS and 10 MHz signal). The clock generation and distribution hardware provides phase-aligned clocks for sampling and signal generation through the Spartan 6 FPGA fabric. The Reference oscillator is also passed on to the RF slice for use in local oscillator generation. Using this scheme, the sampling clock can be set to a maximum of 125 MS/s.

As mentioned previously, the payload supports two primary modes of navigation support. The primary mode for the MAPS mode of operation utilizes a custom header placed within a CCSDS TM packet. This custom header forms the MAPS packet, providing a broadcast capability of payload current time at transmission, position and velocity at a given time, and information about reference frame and uncertainty. The packet itself (including virtual channels, packet counts, and CCSDS headers) are generated by the onboard flight FPGA and provided to the radio for digital processing and baseband transmission. To provide a robust signal, the telemetry output mode utilizes standard error correction capabilities such as: $n=1/2$ Convolutional Encoding Reed Solomon (255, 223), and CCSDS Randomization as seen in Figure 7.

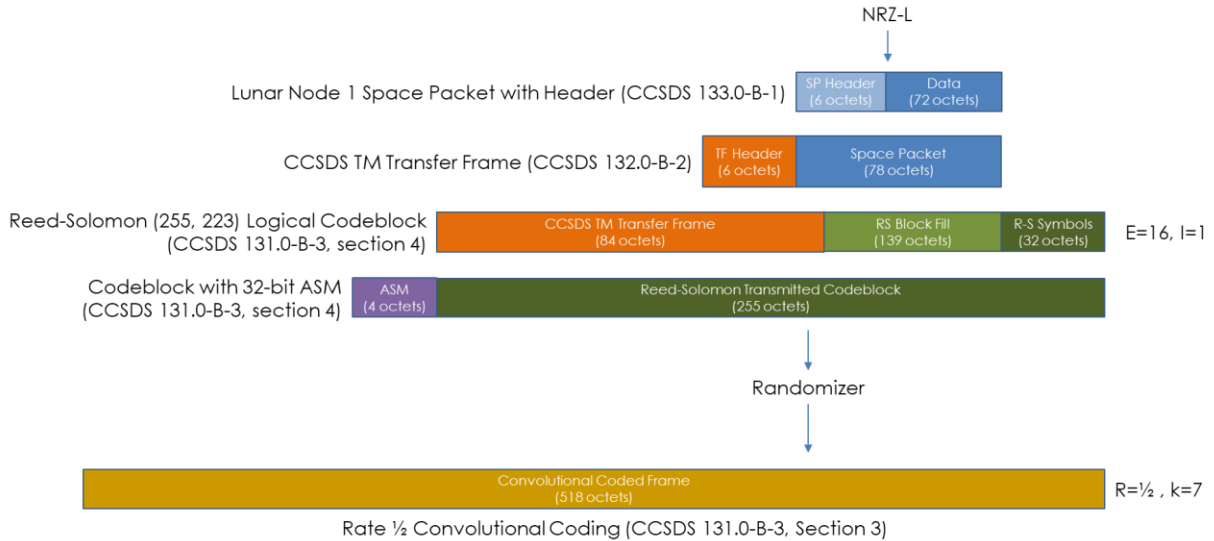


Figure 7. LN-1 Telemetry Format

The radio also includes an implementation of one-way ranging via the JPL ranging code. The PN ranging code generation is accomplished through VHDL code generated using the component code table for the JPL PN Code[1]. The data flow of this process is given in Figure 8 **Error! Reference source not found.**. A pseudo random series of bits are generated by this VHDL code and then applied to the SWIFT SLX constellation modulation block set for BPSK transmission. This block then generates the required I and Q samples to be sent to the digital to analog converter to generate the output signal. This signal is upconverted to the required S-Band frequency using the SLX slice RF frontend which contains an integrated IQ modulator with synthesizer for local oscillator generation and then amplified out to the antenna.

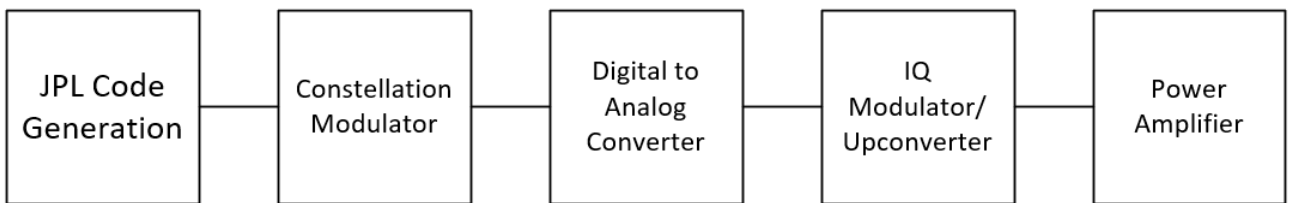


Figure 8. PN Ranging Code Generation and Transmission

GROUND RECEIVER DEVELOPMENT

The previous sections have provided an overview and introduction to the payload itself. In order to demonstrate the navigation functions, Earth-based ground stations will be used to receive and process the measurements, playing the role of the navigating spacecraft. This is used to allow for high fidelity knowledge of the receive location and timing, as well as demonstrating how this capability could be implemented into existing infrastructure. For example, a control network for a network of beacons could utilize Earth-based observations to maintain constellation timing and beacon location. For LN-1, the Deep Space Network is filling this role. This section provides an overview of the ground receiver in use for testing of the

LN-1 payloads as part of DSN RF Compatibility testing. Unique aspects of this test involve using two-way ranging equipment with a received non-coherent one-way signal. The test setup is compared between notional two-way and one-way ranging to provide insight to the configuration changes and operational impacts.

Baseline Two-Way Ranging Approach

The DSN tracking systems contain hardware and software processes to measure 2-way spacecraft range. The ranging hardware and functions are divided between the Uplink Controller (ULC) subsystem that creates the uplink carrier frequency, and the Downlink Channel Controller (DCC) that receives and processes the downlink carrier frequency. The ULC subsystem controls uplink frequency generation, the transmitter hardware, the commanding functions, and the ranging generation functions. The DCC subsystem processes the downlink carrier frequency to measure carrier frequency, which determines the spacecraft Doppler shift and line-of-sight velocity. The DCC subsystem also processes and reports the telemetry modulated onto the downlink carrier, and processes and measures the ranging signal returned from the spacecraft.

The ranging signal path and the DSN hardware used for ranging are shown in Figure 9. The ranging tones are generated within the Uplink Signal Generator controlled by the ULC subsystem. The ranging tones are modulated onto the uplink carrier frequency and transmitted to the spacecraft.

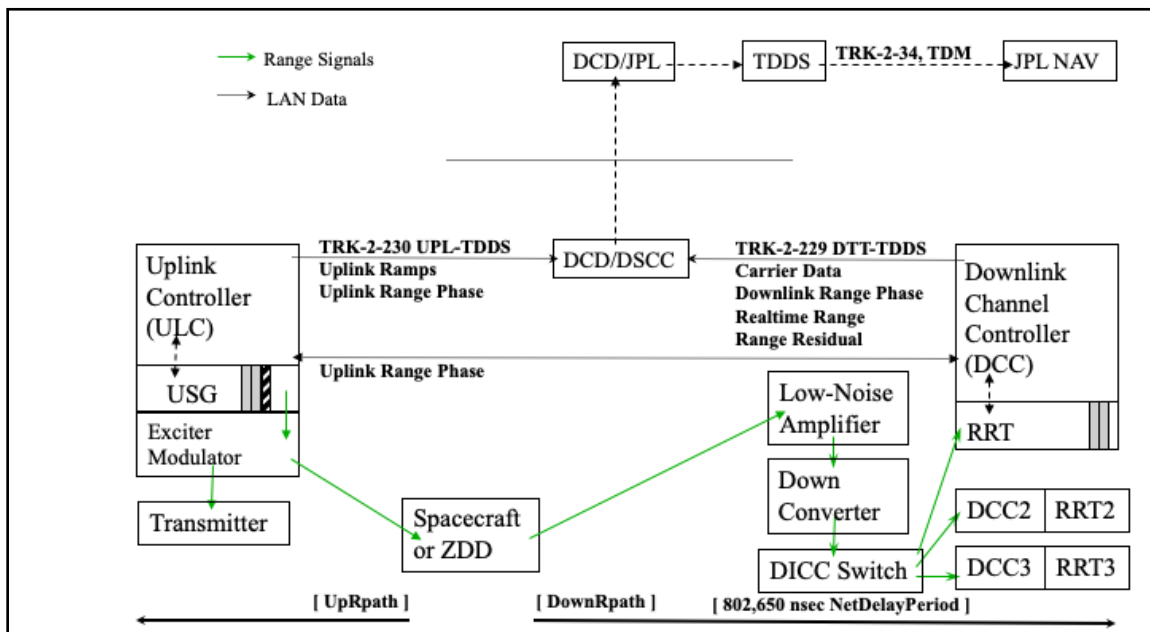


Figure 9. Two-way Ranging Compatibility Testing

Typical spacecraft will acquire the uplink carrier frequency and demodulate the ranging and command signals. The spacecraft will generate a downlink frequency that is coherent with the uplink frequency by multiplying the acquired carrier frequency by a fixed turnaround ratio. The spacecraft may then modulate the downlink frequency with telemetry, and may also modulate the downlink frequency with the ranging signal taken from the uplink carrier. For testing and calibration purposes, the carrier turnaround function can also be performed at a DSN station using a Zero-Delay Device (ZDD) or Uplink Test Translator. This allows the DSN to test and calibrate the ranging system without requiring a spacecraft.

The DCC will acquire and process the downlink carrier frequency returned from the spacecraft. The DCC ranging process relies on the carrier tracking loop to acquire the downlink carrier and then demodulate the ranging signal from the carrier. The ranging processing then samples and integrates the ranging signal. The integrated ranging signal is correlated against a local model of the ranging tones generated within the DCC based on the station timing and reference signals. The DCC produces measurements of the received range phase as a function of time. Independently, the ULC is reporting over the network LAN the generated range phase as a function of time. The DCC computes a realtime 2-way range by subtracting the downlink range phase from the current reported uplink range phase as shown in equations 1 and 2 [11].

$$\text{Realtime Range}(t) = \psi_T(t) - \psi_R(t) \quad (1)$$

Where $\psi_R(t) = \psi_T(t - \text{RTLT}(t))$ (2)

The Realtime Range(t) is the phase delay the range signal experienced over the time RTLT(t).

An important aspect of the DSN ranging measurement technique is that there are no real-time hardware signals that pass directly between the transmitting and receiving equipment. The DCC receiver ranging processing is independent of the uplink hardware and ranging process. The phase of the uplink ranging signal and that of the downlink ranging signal are recorded, and the ranging data are computed from the recorded phases. This implementation provides three advantages.

- 1) This creates a modular design that permits great flexibility. Any DCC receiver works with any antenna, allowing the easy substitution of spare units.
- 2) This allows making three-way ranging measurements in the same way as two-way ranging, except that two ground stations are employed. The DCC receiver does not need to get the signal from the same antenna used for transmitting the uplink carrier signal.
- 3) This allows making one-way ranging measurements on the return link in the same way as two-way ranging. The DCC receiver does not need to know what generated the returned carrier and ranging signal in order to process it.

One-way DSN Ranging Overview

For the three-way and one-way cases, the DCC receiver does not get any real-time information about the reported uplink range phase, because the device (UPL or Spacecraft) generating the ranging signal is not at the same station as the DCC. The one-way ranging configuration is shown in Figure 10.

For these cases, the DCC won't compute a Realtime Range(t). The range must be computed after the fact from the downlink range phase reported by the DCC, using the generated range phase reported by the UPL or Spacecraft. These three-way and one-way cases will report the ranging power and Difference Range Vs Integrated Doppler (DRVID) in real-time. The DRVID is useful for monitoring the consistency of the ranging measurement. The DRVID should have a mean value near zero, and the same variance as the expected variance in the realtime range value.

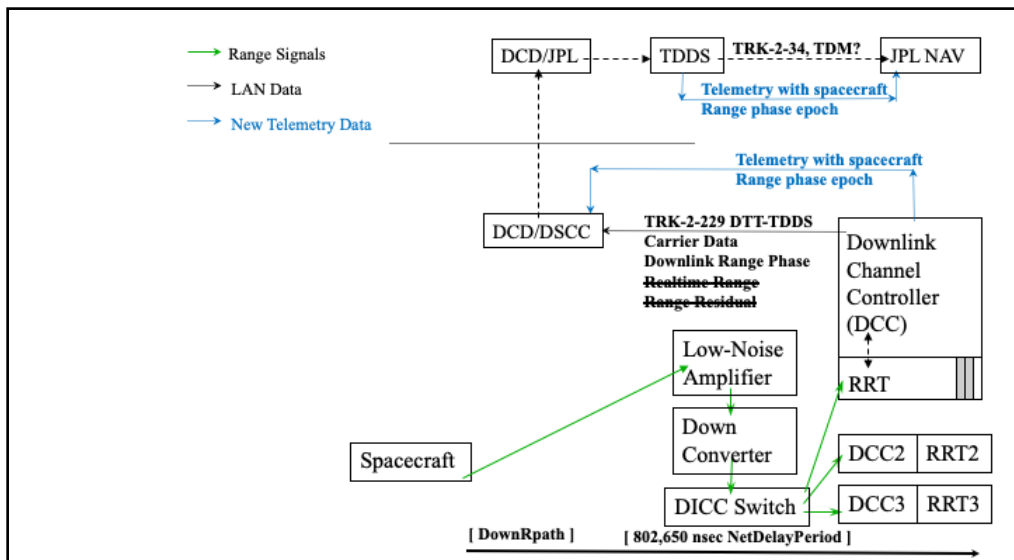


Figure 10. One-way Ranging System Block Diagram

One-way DSN Ranging with UPL Simulated Spacecraft Range

For normal two-way ranging, the generated range phase is produced and reported by the UPL subsystem, and sent to the DCC in a continuous data stream. During one-way ranging, the generated range phase data from the spacecraft is not available to the DCC in realtime. However, a UPL subsystem can be used to simulate the spacecraft generated range during a one-way ranging track. A UPL subsystem must be added to the link and configured to match the ranging configuration onboard the spacecraft. These configuration items are:

- 1) Configure the UPL to the same PN chiprate ratio and PN pattern type as the spacecraft.
- 2) The UPL uplink frequency must be set to the spacecraft transmit frequency (TFREQ) divided by the turnaround ratio used by the spacecraft. This frequency times the correct chiprate ratio will make the UPL produce the same range chiprate as the onboard spacecraft processing.
- 3) Enable ranging on the UPL, to begin sending the uplink range phase data to the DCC.

Figure 11 shows the ranging signal path and the DSN hardware used for simulating the spacecraft range phase during one-way ranging. The advantage of this configuration is that the DCC will produce a range result in realtime, which can be monitored for consistency. This range will have a constant bias from the “true” range, because the generated range produced by the UPL and the onboard spacecraft range are not synchronized to start at the same initial range phase. This bias in the realtime range result will remain fixed during the track, provided the onboard ranging process is not stopped and restarted, and the UPL chiprate frequency matches the onboard ranging chiprate frequency.

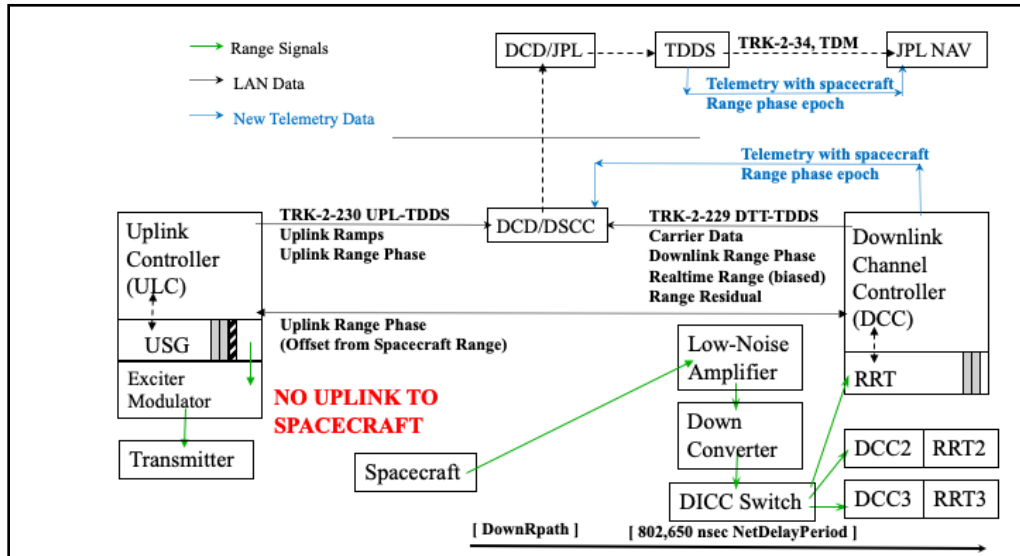


Figure 11. One-way Ranging with UPL Simulated Spacecraft Range

This configuration is useful during initial validation tests to verify the realtime range has the expected variance around the biased realtime range value.

COMPATIBILITY TESTING RESULTS

Given the planned configuration of the ground-receiver to support LN-1 PN Ranging operations, the facility was ready to support DSN RF Compatibility Testing. The LN-1 team traveled with the flight hardware to the DSN EFT-21 test facility. At this location, the payload was put through a range of testing to verify communication linkage decoding, PN performance assessment, and End to End testing with the Mission Operations Center at Marshall Space Flight Center.

Overview of Testing

The LN-1 S-band telecommunications system successfully met all Downlink objectives specified in the official Deep Space Network (DSN) Standard Compatibility Tests. The DSN test facility is equipped with replicas of Deep Space Communication Complex (DSCC) equipment, minus the antenna itself, running the current operational software. A hardline connection mated the LN-1 antenna hat coupler and the DSN receiver equipment.

The vast majority of testing was nominal, aside from the method used for one-way ranging. A new test procedure was created to allow for semi-accurate range measurements with LN-1. This test was deemed to provide acceptable results, as an engineering demo. Other testing included numerous RF link calibrations, downlink spectra inspections and transmitter characterizations.

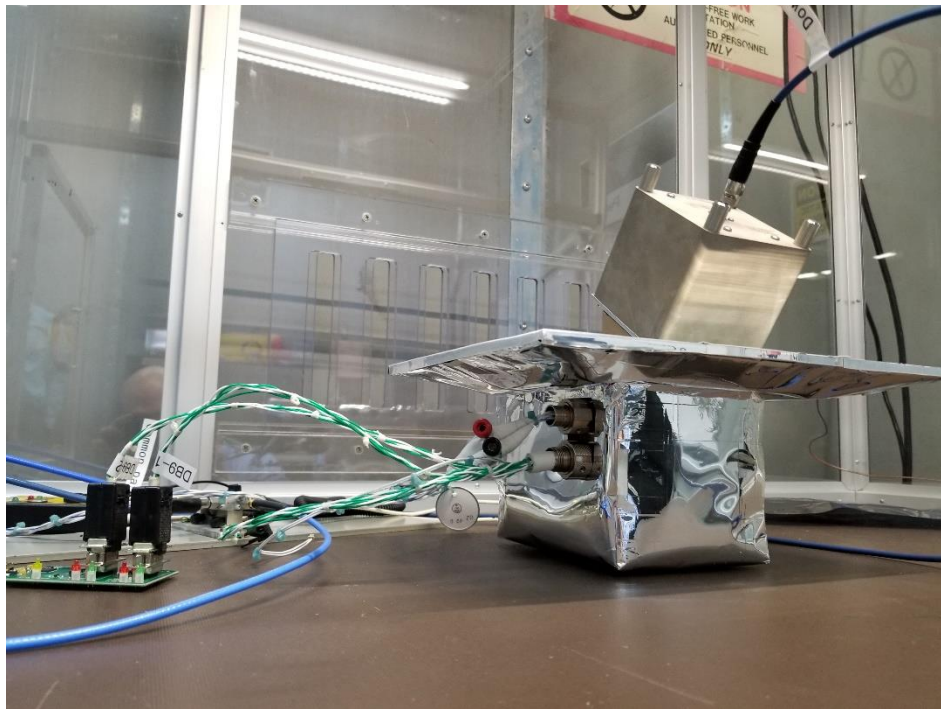


Figure 12. LN-1 at DTF-21

Test Description	# of Configurations	Comment
RFLink Calibrations	1	2x transmitter power configurations.
Downlink Spectra Inspected	3	Carrier-only, Ranging-only, and Telemetry-only configurations were inspected at various frequency spans.
Transmitter Performance Characterizations	1	50 kbps modulated directly onto the carrier.
Range Measurements	3	Data collected with various pattern integration times.

Telemetry Testing

For LN-1 DSN Compatibility Testing, telemetry subsystem functionality and performance were verified. To accomplish this, the DSN receivers were configured to match the LN-1 configurations such that frames can be verified as coming in through the correct virtual channels. The minimum power level (threshold) for error-free telemetry processing was also confirmed. To accomplish this, the power in the link was reduced until errors were observed at the DSN receivers. With the power returned

to threshold, telemetry sampling was performed for a duration sufficient to ensure consistent telemetry processing which meets the specified DSN bit error rate (BER) standard. Around 30.25 Mb of data was sampled error-free.

PN Testing

The secondary objective, as mentioned above, of the testing was to characterize the ability of the payload to generate the PN ranging signal and verify compatibility with the ground receiver. As mentioned previously, the payload has the capability to generate a PN ranging code at a defined chiprate and transmission frequency with a variable sampling rate of applying the code at the chiprate to modulation onto the carrier signal. Figure 13 below provides an overview of where these parameters fit into the ranging signal generation process. Upon command, the payload is configured into the correct mode and waits to begin transmission to the nearest second transition to align the zero phase of the PN code with the second. Given knowledge of the timing onboard the spacecraft (and onboard latency) an estimate can be generated of onboard phase as a function of time. This also results in a bias between the uplink and downlink phases being measured by the DSN equipment and will need to be calibrated out of the system given a known transmission and reception location. The other parameters are used to tweak the generated signal to match ground equipment. This is to match the expected behavior of the ranging setup as described above. For typical DSN ranging, the ground station originates the Uplink tones, which are returned on the Downlink. All downlink data is captured and recorded, but some information can be observed and/or recorded by the link operator. For LN-1 testing, uplink and downlink raw navigation measurements were captured for post-processing.

- Payload generates a PN code to emulate transmission as if the ground system was being “Turned-around” → induces an expected bias
- Optimized uplink frequency, downlink frequency, sampling rate to match behavior of PN generated at notional uplink frequency → tuned to match hardware
- Modified integration time to match observed behavior → frequency errors limit integration time

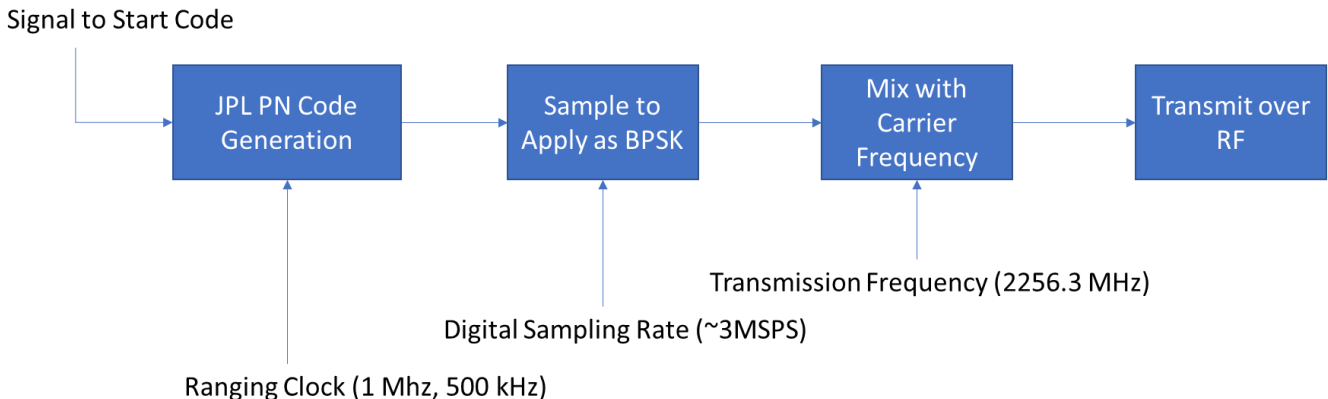


Figure 13. PN Ranging Process Parameters

The testing began by placing the payload into PN transmission mode and assessing the ability to maintain lock with the ranging receiver hardware. This test was conducted late in the day and allowed to continue overnight to assess long-term stability. The initial results of this can be seen below in terms of received frequency and carrier power in Figure 14. As can be seen on frequency, the initial frequency is seen to drift over time as the temperature of the payload stabilize overnight.

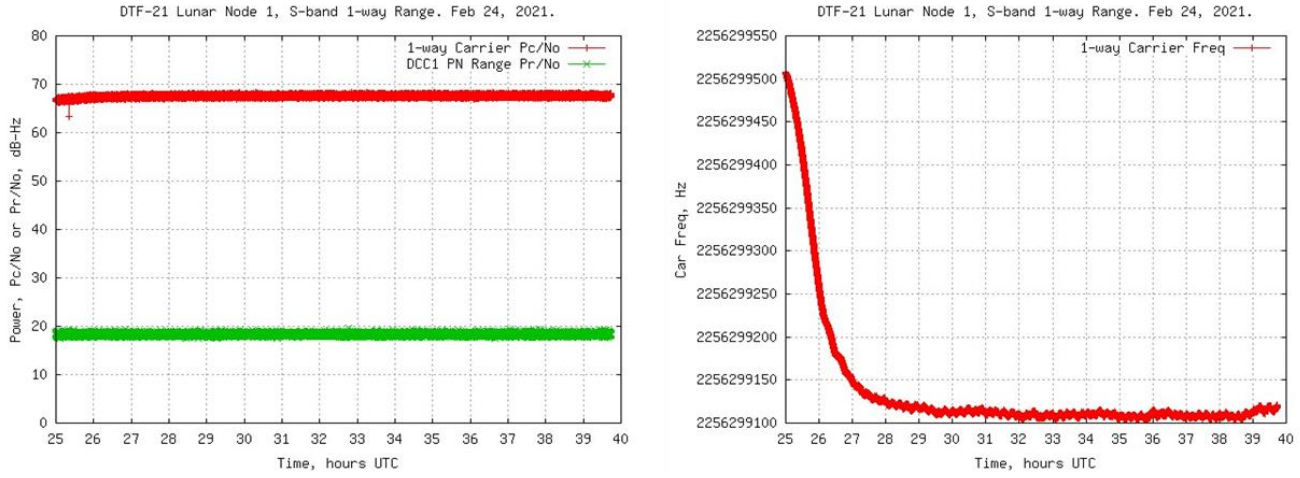


Figure 14. Carrier and PN Power (L), and Carrier Frequency (R) Overnight Test

In order to match assumptions on the ground receiver and simulate the two-way ranging process as described in Figure 11, the radio parameters needed to be tweaked to maximize the measured power on the ranging signal. This involved implementing the turn-around ratio (240/221) as a combination of transmission frequency tweaks and chiprate tweaks to the transmission. Similarly, the sampling frequency was increased to allow for the maximum resolution of the signal generation. This process required iteration between the radio parameters and those used on the ground-generated uplink, i.e. signal frequency to maximize the PN power. For example, over the course of this iteration, the uplink frequency was optimized to 2,077,675,710 Hz with a chiprate = 2,028,980.18555 Hz to match the radio's resolution on generation of the 2256.3 MHz downlink carrier and 2 MHz chiprate. In addition to this, the integration was set to a low value (5 seconds). The resulting range measurement (to the generated uplink signal) is given in Figure 15. As seen in this picture, the results showed the expected large bias due to the non-coherence, but also showed a constant steady growth in measured range over the course of the night at a seemingly linear rate.

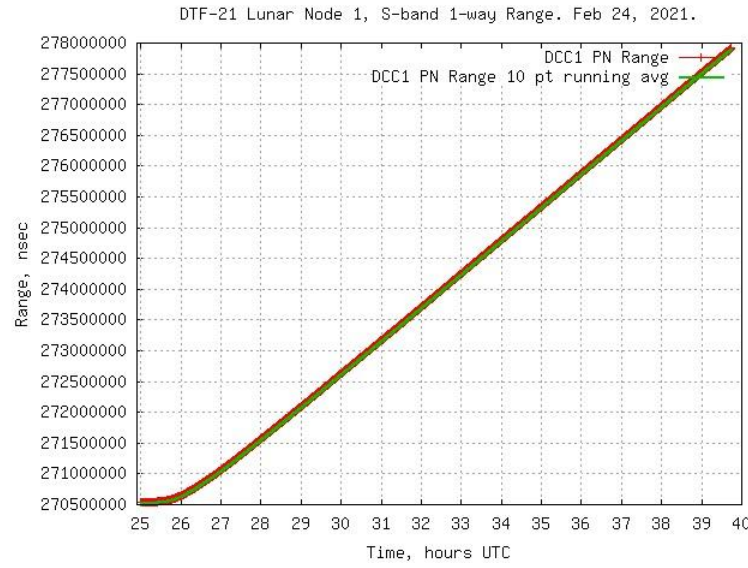


Figure 15. Measured Range

This behavior can also be seen in the measurements of DRIVD and range delta over time as seen in Figure 16. The left chart shows the difference between the computed range from the Doppler observation (the expected vs received downlink frequency) and the computed change in range in Range Units. The results show a fairly linear offset over the course of the mission. For a static scenario this value would be centered near zero, with the noise capturing the measurement uncertainty. This can also be

seen in the right image showing the difference between subsequent range errors that as the frequency stabilized, so too did the range delta. This represents the behavior being a function of the carrier downlink frequency stability, and can be correlated with a frequency drift of 400Hz exhibited over thermal stabilization.

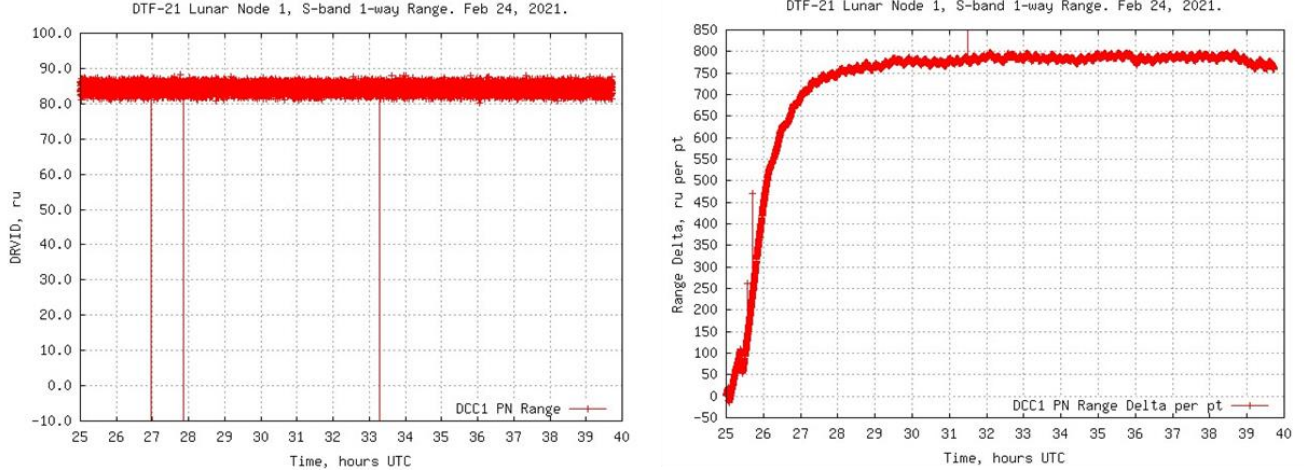


Figure 16. DRVID (L) and Delta Range (R)

This behavior is more clear in Figure 17 below. The plot in red is the carrier residual (change in frequency) from the nominal and the green curve is the range delta per point. The scaling has been applied to the range delta to focus on this visualizing the trend. As seen the two curves dynamic behavior is tightly coupled over the course of the test. This shows the relationship between the transmission frequency error and range error, which effectively acts as noise on the range measurement. This function shows that as the frequency changes so does the chiprate and the resulting error can be seen.

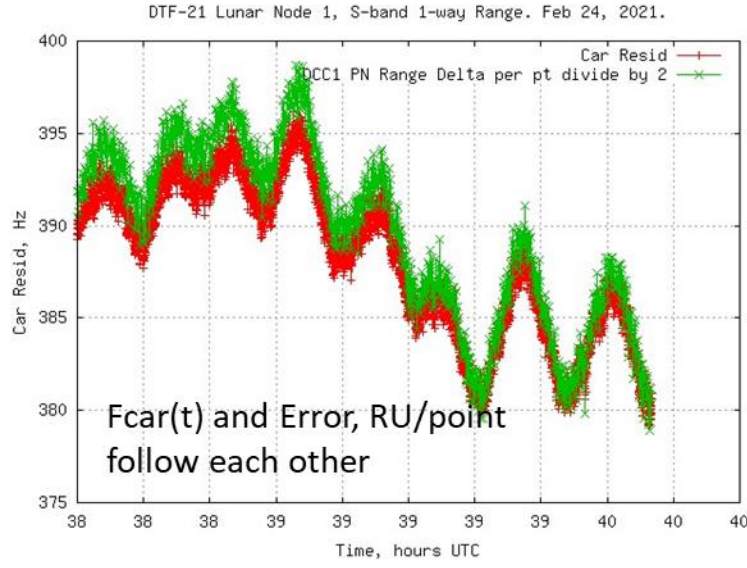


Figure 17. Dynamic Behavior of Error and Residual

The fixed offset in DRVID also points to another concern. This error is directly tied to an offset between the expected and actual chiprate being transmitted, i.e. something separate from the carrier frequency drift. The error can be calculated by existing methods[12], given the DRVID value, the turn-around ratio, and the integration time. For this scenario, the Ferror was calculated to be 33.6 Hz. Due to the DRVID being non-zero, the error can be attributed to errors in the generated signal. Here it's important to note that to mimic the turn-around signal, the turn-around is applied by modifying the transmission frequency. This frequency error is a small portion of the transmission frequency of 2256299500 Hz (the tweaked value to maximize PN ranging power). This equates to essentially one bit in 2^{26} , approximately 1.5×10^{-8} Hz. If one calculates the turn-around ratio (221/240) as a single precision float, the precision will result in a rounding error of 1.58946×10^{-8} , and a resulting equivalent

Ferror of 35.86 Hz. This would cause a DRVID error 82.6 RU, which is very close to what is seen in the experimental results. As such, this error can be traced back to the precision of the radio's process for generating the chipset and output frequency. This behavior was also evident in the initial tuning that limited the precision of modifications to the transmission frequency to precisely match a turn-around from a defined uplink. This performance can be improved by modification of the radio's firmware to support a higher precision float used for generation of the PN code. This has been implemented and initially tested. In order to meet flight deliveries and to maintain firmware matched between flight and DSN testing, the flight radio's firmware was not updated with this change. However, this update will be implemented on a second transceiver that will enable selection of the precision used in PN code generation. With this unit, the team will conduct additional ground testing and be able to verify this relationship and correct the static DRVID.

This error in chiprate also had an impact on the integration time, which can be used to reduce noise on the observed phase. For the ground testing, an integration time of 5 seconds was used. Typically, larger values are used to reduce noise, especially for low power signals. This integration time has an upper limit defined by analysis in [12] as being a function of the Ferror term. This process works in the following steps 1. The Ferror causes the receiver integration to compute an Fchip and sampling frequency that is slightly wrong. 2. The longer it integrates with this wrong sampling frequency, the more out-of-phase the ranging accumulation. 3. When the DRVID error goes past $\frac{1}{2}$ the Range Clock tone (512 RU), the accumulation is now destructively interfering the range signal. As such, this sets a maximum integration time of 33 seconds.

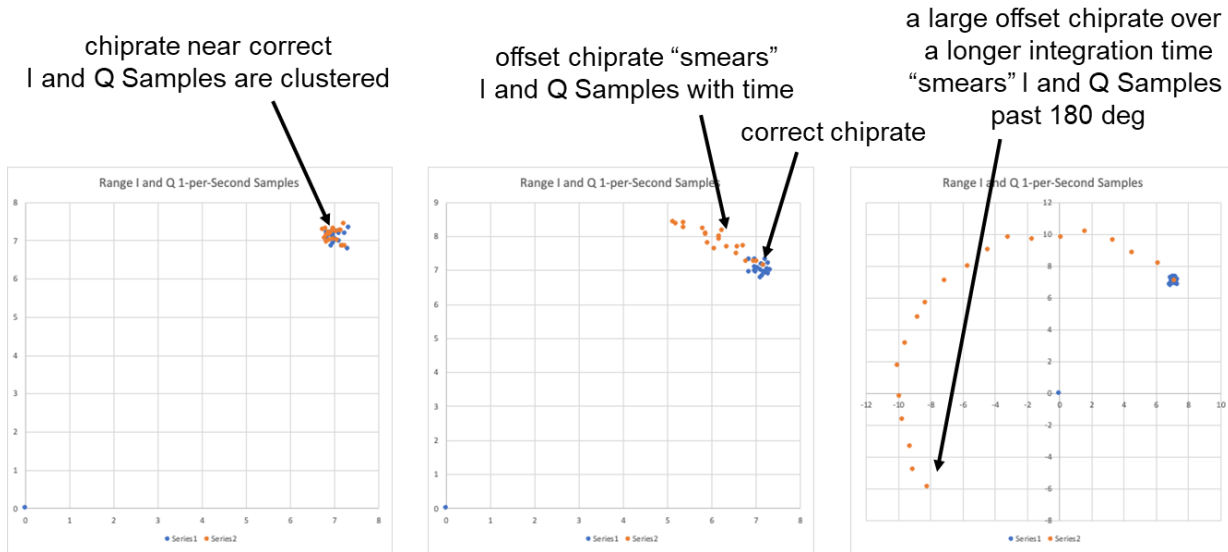


Figure 18. Impact of Ferror on PN Measurement

Due to this smearing behavior the project has to trade between the impacts of noise and smearing. This resulting in a selection of a 5 second integration. As part of the compatibility testing, the team did test multiple integration times include 3, 10, and 30 seconds to assess performance impacts. The results are shown in Figure 19. This test was performed with a fixed duration at each integration interval resulting in fewer points at longer settings. The results show that the impact of the smearing on the DRVID results, showing how this smearing impacts how far the range measurement smears over each, and showing consistent behavior between measurements.

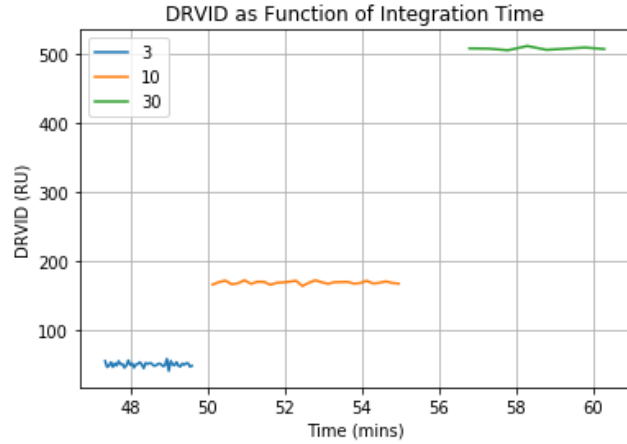


Figure 19. Impact of Integration Time on DRVID

Flight Operations Approach

The results of this analysis and the ground testing both are informing how operations will be conducted during flight. As seen in the previous sections, LN-1 is expected to have a large offset bias and range ramp rate in any navigation measurement. The team is continuing to mature the analysis tools to take advantage of the collected observations to develop advanced flight-like error models with application to the lunar determination case with full dynamic modeling. This is being developed using the MONTE suite to refine the analysis scenario and use in flight operations to track operational performance.

The range bias is primarily a function of the offset between the LN-1 clock and NOVA-C clock. This delta will be present in both MAPS and PN-based navigation (though not Doppler tracking). This is limited operationally by the host vehicle's approach to time synchronization. Upon landing and during mission operations, clock offset information will be provided to LN-1 to correct for the broadcast timestamp (and initial ranging phase bias) via ground-based corrections. Similarly, characterizations are being performed to capture the latency of LN-1 updating its clock when synced to the lander as well as the internal communication latency from packet generation to transmission. This directly ties into one of the trades being assessed as part of the flight experiment: long-term stability of each ranging signal and the need for calibration.

Currently, operations are being planned to include roughly 1 hour of ground observation during cruise to lunar orbit, and then 8-12 hours of day of ground site scheduling during lunar surface operations. During cruise, the payload is focusing on collecting telemetry information (MAPS) as well as Doppler tracking information. This focus is due to the limited time available for passes, as well as the limited operational time. For example, it is not expected that the payload will have adequate time to warm up and produce a frequency stable enough for the navigation measurement via PN ranging. While on the lunar surface, the team will exercise both operational modes of navigation in order to assess stability and performance. In contrast to cruise operations, the payload will remain powered on while on the surface. This will allow the ground station to take some observations and then wait until the next pass, when the payload should still be in the same operational state. This will allow for assessments of stability over a longer time period without needing a long duration ground pass (which is difficult to attain due to heavily utilized ground assets). With this setup, the team is hoping to capture long-term system stability and maintain the radio in a frequency-stable state to remove the impact of transmission frequency drift due to onboard temperature behavior from the navigation analysis. These passes will be split between PN and MAPS passes to both collect timing stability of the LN-1 clock as well as the long-term frequency stability of transmitted PN code. During the PN passes, raw intermediate frequency (IF) data will be collected for further processing and analysis.

The operational approach of LN-1 will also allow for comparison between multiple disparate navigation approaches, enabling comparison of independent solutions. Similarly, the host vehicle will provide independent solutions of the lander location during lunar cruise and on the surface to serve as a best estimate. The team will use PN and MAPS time-transfer measurements to perform range-based determination of the landing location. Similarly, the team will also perform state estimation using only Doppler observations. One key metric that will be assessed is the required frequency of re-calibration through post-processing, to assess the growth of uncertainty over time of the navigation solution as well as selecting pieces of data to use as calibration given the best estimate location (using all navigation data during the landed portion) to provide

insight into the operational requirements of a planetary beacon, providing a parallel to the ground control network for a terrestrial Global Navigation Satellite System. The team is also pursuing partnerships to also collect Very Long Baseline Interferometry observations as a third independent source (in addition to the DSN-based LN-1 observations, and lander provided navigation solution).

SUMMARY AND CONCLUSIONS

These results are driving the forward work of the team ahead of flight. The primary need is to develop an error model that accurately captures the behavior of the ranging signal over time. Analysis tools are being set up to simulate ranging and Doppler measurements for the flight scenario and will be used to provide pre-flight estimates of the navigation accuracy. This will enable assessment of the ability of orbit determination algorithms to operate under large bias and range ramp rates. The results of this will be presented in future publications. Additionally, the team has procured a second flight-like radio with firmware updates improving the onboard precision. With this radio, the team will conduct additional ground testing to verify the impact of this decimation on the measured downlink phase and DRVID observations. This testing is currently slated for Spring 2022. Additional testing will ascertain the capability of the system at multiple transmission frequencies as well as transmission rates without the constraint of the turn-around ratio to reduce the impact of the decimation. This testing will continue through flight to provide additional insight to the performance of the system. Post-mission the observational results will be used to inform future beacon developments and provide error models that can guide future architecture assessments. Similarly, the LN-1 team is continuing to mature this approach with Lunar Node -2 proposals. The next iteration of the hardware is planned to include two-way capabilities with focused updates based on these results.

This article provides a summary of the Lunar Node -1 mission and its approach to enabling future techniques and architecture development for in-situ navigation at the moon. The payload is slated to fly to the moon on the NOVA-C lander mission in 2022. The results of DSN RF Compatibility testing have been provided to show functional testing between the payload and ground receivers. Similarly, the PN-based ranging characterization provides valuable insight to the challenges of non-coherent one-way ranging. Other systems have focused on having the s/c being a one-way receiver vs. transmitter[13,14], and each has their unique constraints (transmit gain vs receive gain, onboard clock stability, onboard computing capability, etc. The results indicate the sensitivity of the uplink ranging phase to onboard decimation, as well as the strong impact of thermal stability of the generated signal. The team continues to assess the impact of these to orbit determination performance for multiple mission scenarios to demonstrate the capability of this navigation approach.

ACKNOWLEDGMENTS

The authors would like to acknowledge the support of our management across multiple organizations including Marshall Space Flight Center, the Jet Propulsion Laboratory, and Peraton, Inc. Lunar Node -1 is funded as a part of the NASA-Provided Lunar Payloads program operated from NASA's Science Mission Directorate. The LN-1 authors would also like to express our gratitude to the rest of the engineering, design, support, and implementation team at Marshall Space Flight Center who were critical to making this project a reality.

REFERENCES

1. Smith, Marshall, et al. "The Artemis Program: An Overview of NASA's Activities to Return Humans to the Moon." 2020 IEEE Aerospace Conference. IEEE, 2020.
2. Hooke, A. "The interplanetary internet." Communications of the ACM 44.9 (2001): 38-40.
3. Israel, D. J., et al. "Luna net: a flexible and extensible lunar exploration communications and navigation infrastructure." 2020 IEEE Aerospace Conference. IEEE, 2020.
4. Wollenhaupt, W. "Apollo orbit determination and navigation." 8th Aerospace Sciences Meeting. 1970.
5. Nicholson, A., et al. "NASA GSFC lunar reconnaissance orbiter (LRO) orbit estimation and prediction." SpaceOps 2010 Conference Delivering on the Dream Hosted by NASA Marshall Space Flight Center and Organized by AIAA. 2010.
6. Anzalone, E., et al. "Multi-Spacecraft Autonomous Positioning System: Low Earth Orbit Demo Development and Hardware-in-the-Loop Simulation." Annual AIAA/USU Conference on Small Satellites. No. M15-4828. 2015.
7. Anzalone, E., Becker, C., and Sims, H.. "Initial Results of the Software-driven Navigation for Station Experiment." 2018 AIAA SPACE and Astronautics Forum and Exposition. 2018.
8. Anzalone, E., Iyer, A., and Statham, T. "Use of Navigation Beacons to Support Lunar Vehicle Operations." 2020 IEEE Aerospace Conference. IEEE, 2020.

9. Evans, S., et al. "MONTE: The next generation of mission design and navigation software." *CEAS Space Journal* 10.1 (2018): 79-86.
10. O'Dea A., Pham T., Kinman P., Chang C., "214 Pseudo-Noise and Regenerative Ranging," DSN No. 810-005, 214, Rev. A, October 28th 2015, pp. 9-11.
11. Berner J., Bryant S., and Kinman P., "Range Measurement as Practiced in the Deep Space Network", Proceeding of the IEEE, Vol 95, No. 11, November 2007.
12. Reynolds, M., et al. "A two-way noncoherent ranging technique for deep space missions." *Proceedings, IEEE Aerospace Conference*. Vol. 3. IEEE, 2002.
13. T. A. Ely, E. A. Burt, J. D. Prestage, J. M. Seubert, and R. L. Tjoelker, "Using the deep space atomic clock for navigation and science," *IEEE transactions on ultrasonics, ferroelectrics, and frequency control*, vol. 65, no. 6, pp. 950–961, 2018.
14. Ely, T. A., and Seubert, J. "One-way radiometric navigation with the deep space atomic clock." *AAS/AIAA Space Flight Mechanics Meeting*. 2015.